

Cite this: *RSC Adv.*, 2018, 8, 29967

# Identification of 4-isopropyl–thiotropolone as a novel anti-microbial: regioselective synthesis, NMR characterization, and biological evaluation†

 Mohamed Elagawany,<sup>ab</sup> Lamees Hegazy,<sup>a</sup> Feng Cao,<sup>c</sup> Maureen J. Donlin,<sup>d</sup>  
 Nigam Rath,<sup>e</sup> John Tavis<sup>f</sup> and Bahaa Elgendy<sup>id</sup>\*<sup>ag</sup>

We have synthesized and separated tosylated thujaplicin isomers for the first time, and elucidated their structures using 1D, 2D-NMR techniques and X-ray crystallography. The tosylated isomers were used to synthesize 4-isopropyl–thiotropolone and 6-isopropyl–thiotropolone in a regioselective manner. <sup>1</sup>H and <sup>13</sup>C Chemical shifts of synthesized isomers were fully assigned using several NMR experiments, and their isotropic magnetic shielding was calculated using the GIAO (Gauge Including Atomic Orbitals) method and the B3LYP def2-TZVPP level of theory. The calculated chemical shift values were in a good agreement with the experimental results. The biological activity of all synthesized compounds was evaluated against the fungal pathogen *Cryptococcus neoformans* and four different bacterial strains (*Staphylococcus aureus* (ATCC 29213), *E. coli* (ATCC 35218), *Acinetobacter baumannii* and *Pseudomonas aeruginosa* (ATCC 27853)). 4-Isopropyl–thiotropolone was found to inhibit *Staphylococcus aureus* in a low micro molar range and exhibit good therapeutic index and ADME properties. This compound can be used for future lead optimization to design inhibitors against *Staphylococcus aureus* (ATCC 29213).

Received 25th July 2018  
Accepted 20th August 2018

DOI: 10.1039/c8ra06297h

rsc.li/rsc-advances

## Introduction

The troponoid core is well known in hundreds of natural products. The tropone ring has a unique structure and properties and despite their non-benzenoid nature, they are planar and possess aromatic character. Natural and synthetic compounds that have the troponoid core have profound biological activities and have been used as antitumor,<sup>1–3</sup> antifungal,<sup>4</sup> and antimicrobial agents.<sup>5</sup> The biological activities of these compounds has been mainly attributed to their inhibitory effect on bimetallic enzymes.<sup>6,7</sup> Colchicine (**1**) is the most recognized member of this family because it has been used for the treatment of gout<sup>8</sup> and

familial Mediterranean fever<sup>9</sup> since the time of ancient Egyptians.<sup>10</sup> Hinokitiol ( $\beta$ -thujaplicin) (**2**) is among the known tropolone derivatives that showed inhibitory effects against *Chlamydia trachomatis* and has clinical potential to be used as a topical drug to prevent sexually transmitted diseases.<sup>11</sup>

Thiotropolones have not been widely explored compared to structurally related hydroxytropolones. Some examples exist in literature that shows anticancer activity such as thiocolchicin (**3**), which can act as tubulin<sup>12</sup> or topoisomerase II inhibitor.<sup>13</sup> Thiotropocin (**4**) is another structurally related antibiotic that was isolated from *Pseudomonas* sp. CB-104 in 1984.<sup>14,15</sup> This antibiotic was found to exhibit antibacterial, antifungal, and antiprotozoal activities *in vitro*. Recently, Donlin and co-workers<sup>4</sup> reported that thiotropolone **5** can inhibit the growth of the fungus *Cryptococcus neoformans* with a minimal 80% inhibitory concentration (MIC<sub>80</sub>) of 0.25  $\mu$ M. In our effort to design and synthesize new thiotropolones to treat pathogenic fungi and multidrug resistant bacteria, we used the natural product  $\beta$ -thujaplicin (**2**) as starting point (Fig. 1).

Here, we report for the first time the isolation of the intractable mixture of tosylated thujaplicines, **8** and **9**, their full NMR assignments and the X-ray structure of **8**. Moreover, we report the synthesis, full NMR chemical shift assignments of 4-isopropyl and 6-isopropyl-2-mercaptocyclohepta-2,4,6-trien-1-one, **10** and **11**, and their anti-*Cryptococcus neoformans* and antibacterial activity. Moreover, we have evaluated the ADME (adsorption, distribution, metabolism, excretion and toxicity) properties of tested compounds.

<sup>a</sup>Departments of Pharmacology and Physiology, Saint Louis University School of Medicine, St. Louis, MO, USA

<sup>b</sup>Department of Pharmaceutical Chemistry, Faculty of Pharmacy, Damanhour University, Damanhour, Egypt

<sup>c</sup>John Cochran Division, Department of Veteran's Affairs Medical Center, 915 North Grand Blvd., St. Louis, MO 63106, USA

<sup>d</sup>Edward A. Doisy Department of Biochemistry and Molecular Biology, Saint Louis University School of Medicine, St. Louis, Missouri, USA

<sup>e</sup>Department of Chemistry and Biochemistry, Center for Nanoscience, University of Missouri – St. Louis, One University Boulevard, St. Louis, USA

<sup>f</sup>Department of Molecular Microbiology and Immunology, The Saint Louis University Liver Center, Saint Louis University School of Medicine, St. Louis, Missouri, USA

<sup>g</sup>Chemistry Department, Faculty of Science, Benha University, Benha 13518, Egypt. E-mail: belgendy@fsc.bu.edu.eg

† Electronic supplementary information (ESI) available. CCDC 1856450. For ESI and crystallographic data in CIF or other electronic format see DOI: 10.1039/c8ra06297h



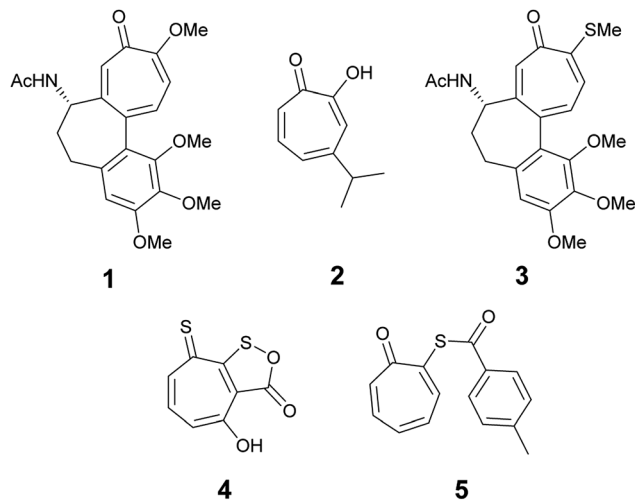


Fig. 1 Examples of biologically active tropolones.

## Results and discussion

Tosylation is usually the first step toward functionalization of hydroxytropolones to prepare biologically active derivatives. Under standard conditions of tosylation, where base is used in excess, the formed anion of unsymmetrical hydroxytropolones (Fig. 2A) undergoes isomerization to give a mixture of isomers. During their attempt to synthesize *O*-alkyl derivatives of 4-isopropyl-tropolone as ribonucleotide reductase inhibitors, Crozet and his co-workers<sup>16</sup> observed the formation of a mixture of 4- and 6-isopropyl derivatives (1 : 1 mixture). They were only able to obtain sufficient amounts of the 4-isopropyl derivatives in a pure form suitable for testing. Similarly, tosylation of colchicine (1) gave the biologically inactive 9-tosyloxycolchicide isomer (6) as the major product ( $\approx 74\%$ ) while the biologically active 10-tosyloxycolchicide isomer (7) was the minor product ( $\approx 26\%$ ).<sup>17</sup>

Tosylated thujaplicines, **8** and **9**, are important synthetic intermediates in the synthesis of many biologically active tropolones. For example, they were used as an intermediate in the preparation of copper aminotropones, which were found to be more effective than a commercial toothpaste formulation in inhibiting plaque formation.<sup>18</sup> The inability to separate **8** and **9** and their use as a mixture of isomers complicates the purification of the desired ligands. Obtaining such mixture of isomers is undesirable, and selective tosylation or facile separation of isomers is crucial from the synthetic point of view.<sup>18</sup>

Hinokitiol ( $\beta$ -thujaplicin) (**2**) was treated with *p*-toluenesulfonyl chloride in presence of pyridine in dichloromethane (DCM) at room temperature to give a mixture of 5-isopropyl-7-oxocyclohepta-1,3,5-trien-1-yl-4-methylbenzenesulfonate (**8**) and 3-isopropyl-7-oxocyclohepta-1,3,5-trien-1-yl-4-methylbenzenesulfonate (**9**) in  $\approx 1 : 1$  ratio. The isolation of this mixture was reported to be intractable.<sup>19</sup> To obtain **9** (the isomer of the natural product) exclusively, it has to be through multistep synthesis. The first step involves iodination of **2** in position 7 followed by tosylation of hydroxyl group at position 2. The final step is to remove the iodine

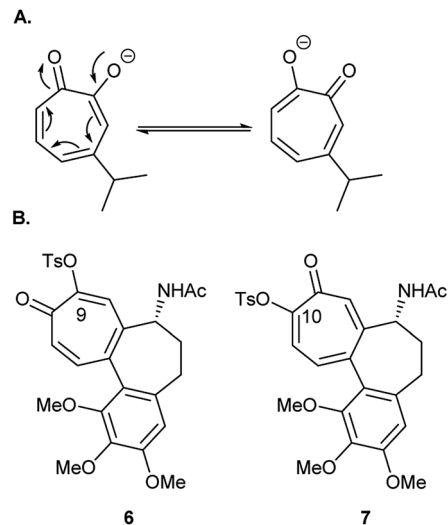
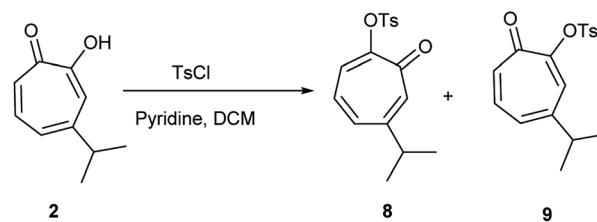


Fig. 2 (A)  $\beta$ -Thujaplicin anions. (B) Tosyloxycolchicides **6** and **7**.



Scheme 1 Synthesis of compounds **8** and **9**.

by hydrogenation using Pd/C (10%) in presence of anhydrous sodium acetate.<sup>19</sup> Nevertheless, we were able to separate the two isomers using a Reveleris X2 flash chromatography system. The structures of **8** and **9** (Scheme 1) were elucidated using 1D and 2D NMR spectroscopy and single crystal X-ray diffraction.

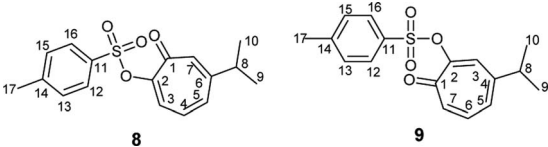
Compound **8** was obtained as colorless sharp needles. Its molecular formula  $C_{17}H_{18}O_4S$  was determined by HRESIMS data ( $m/z$  341.0816  $[M + Na]^+$ , calc. 341.0818). The analysis of  $^1H$ ,  $^{13}C$ , COSY, HSQC, and HMBC spectra revealed the presence of a singlet proton H-7 ( $\delta_C/\delta_H$  137.7/7.05, C-7). This proton shows two bond correlations with C-1 ( $\delta_C$  179.1) and C-6 ( $\delta_C$  157.3) and strong three bond correlations with C-2 ( $\delta_C$  154.5) and C-8 ( $\delta_C$  38.3). Furthermore, the one methine septet H-8 ( $\delta_C/\delta_H$  38.3/2.73, C-8) shows two bond correlations to C-6 and three bond correlations to C-7. The two-methyl doublet  $H_3-9$  and  $H_3-10$  ( $\delta_C/\delta_H$  22.6/1.17, C-9 and C-10) shows a strong three bond correlation to C-6. H-4 ( $\delta_C/\delta_H$  129.1/6.88, C-4) shows strong three bond correlations to C-2 and C-6, which further confirms the location of tosyl and isopropyl groups (Table 1).

We have calculated both  $^1H$  and  $^{13}C$  isotropic chemical shielding of **8** at the B3LYP/def2-TZVPP level of theory. Correlation plots between experimental and calculated chemical shifts shows very good correlations with correlation coefficients ( $R^2$ ) of 0.9946 and 0.9755 for  $^{13}C$  and  $^1H$  NMR chemical shifts, respectively (Fig. S50†).

Compound **9** was obtained as a white powder. Its molecular formula  $C_{17}H_{18}O_4S$  was determined by HRESIMS data ( $m/z$



**Table 1** Experimental and calculated  $^1\text{H}$  and  $^{13}\text{C}$  isotropic chemical shifts (ppm) of compounds **8** and **9**<sup>a</sup>



Atom	$\delta_{\text{Exp}}$ <b>8</b>	$\delta_{\text{Calc}}$ <b>8</b>	$\delta_{\text{Exp}}$ <b>9</b>	$\delta_{\text{Calc}}$ <b>9</b>
C-1	179.1	188.9	178.9	189.1
C-2	154.5	173.1	154.6	171.4
C-3	129.2	140.9	131.7	145.6
C-4	129.6	142.1	152.4	167.8
C-5	136.6	143.4	130.5	138.2
C-6	157.3	167.1	137.0	144.5
C-7	137.7	155.5	138.9	152.4
C-8	38.3	51.2	38.0	48.1
C-9 and C-10	22.6	28.9	22.7	28.3
C-11	133.4	151.9	133.4	151.7
C-12 and C-16	128.4	141.4	128.5	141.4
C-13 and C-15	129.2	138.5	129.6	138.7
C-14	145.3	157.3	145.6	157.2
C-17	21.7	27.3	21.8	27.4
H-3	7.29	8.12	7.36	8.31
H-4	6.88	7.69	—	—
H-5	6.98	7.73	6.93	7.68
H-6	—	—	7.14	7.94
H-7	7.05	8.23	7.02	8.044
H-8	2.73	3.47	2.80	3.64
H-9 and H-10	1.17	2.01	1.21	2.05
H-12 and H-16	7.89	10.15	7.90	10.07
H-13 and H-15	7.31	8.27	7.33	8.28
H-17	2.42	3.35	2.43	3.3445

<sup>a</sup>  $^{13}\text{C}$  assignments were based on HSQC and HMBC spectra.  $^1\text{H}$  assignments were based on 1D- $^1\text{H}$  NMR and COSY spectra.

341.0818  $[\text{M} + \text{Na}]^+$ , calc. 341.0815). The analysis of  $^1\text{H}$ ,  $^{13}\text{C}$ , COSY, HSQC, and HMBC spectra revealed the presence of a singlet proton ( $\delta_{\text{C}}/\delta_{\text{H}}$  131.7/7.36, C-3). This proton shows two bond correlations with C-2 ( $\delta_{\text{C}}$  154.5) and C-4 ( $\delta_{\text{C}}$  152.4) and strong three bond correlations with C-1 ( $\delta_{\text{C}}$  178.9) and C-8 ( $\delta_{\text{C}}$  38.0). Furthermore, the one methine septet H-8 ( $\delta_{\text{C}}/\delta_{\text{H}}$  38.0/2.80, C-8) shows two bond correlations to C-4 ( $\delta_{\text{C}}$  152.4) and three bond correlations to C-3. The two-methyl doublet  $\text{H}_3\text{-9}$  and  $\text{H}_3\text{-10}$  ( $\delta_{\text{C}}/\delta_{\text{H}}$  22.7/1.21, C-9 and C-10) shows a strong three bond correlation to C-6. H-6 ( $\delta_{\text{C}}/\delta_{\text{H}}$  137.0/7.14, C-6) shows strong three bond correlations to C-1 and C-4, which further confirms the location of carbonyl and isopropyl groups. Besides, H-7 ( $\delta_{\text{C}}/\delta_{\text{H}}$  138.9/7.02, C-7) shows a strong three bond correlation to C-2, which confirms the position of tosyl group (Table 1).

We have calculated both  $^1\text{H}$  and  $^{13}\text{C}$  isotropic chemical shielding of **9** at the B3LYP/def2-TZVPP level of theory. Correlation plots between experimental and calculated chemical shifts shows very good correlations with  $R^2$  of 0.9962 and 0.9789 for  $^{13}\text{C}$  and  $^1\text{H}$  NMR chemical shifts, respectively (Fig. S51†).

Our NMR assignments were further confirmed by obtaining an X-ray crystal structure of compound **8** (Fig. 3). The X-ray shows that the tosyl group is in position 2 while isopropyl

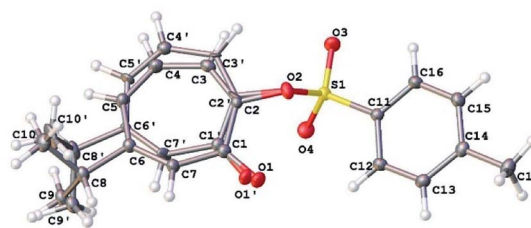


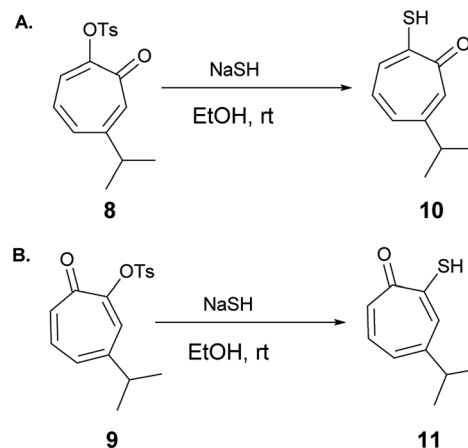
**Fig. 3** X-ray crystal structure of compound **8** showing the atom-numbering scheme.

group is in position 6 of the tropolone ring. Compound **8** was crystallized from ethyl acetate (0.2 mL), ether (0.5 mL), and hexanes (10 mL) by solvent evaporation. Crystallographic data is given in Table S1.† The crystals of compound **8** crystallize in the monoclinic space group  $P2_1/c$  with four molecules in the unit cell ( $Z = 4$ ) of dimensions  $a = 5.62$ ,  $b = 28.31$ ,  $c = 9.51$  Å and  $\beta = 92.4^\circ$ .  $V = 1512.31(11)$  Å<sup>3</sup>.

The 7-membered ring is disordered over 2 orientations (80 : 20%). The disorder was modelled with partial occupancy atoms and it indicates that the 7-membered ring was “breathing” by moving from less hindered to more hindered confirmation which facilitate the migration of tosyl group in substitution reactions. The tosyl group in **8** and **9** were shown to be fluxional and undergo thermally-induced shift between the two thujaplicin oxygen atoms. Molecular mechanics calculations by the MMFF94 force field suggests that this process takes place most likely through bipyramidal intermediate.<sup>20</sup>

6-Isopropyl-thiotropolone (**10**) and 4-isopropyl-thiotropolone (**11**) were readily accessible in good yields by reacting **8** and **9** with sodium hydrosulfide in ethanol at room temperature (Scheme 2). The structures of **10** and **11** were fully assigned using 1D and 2D NMR spectroscopy.

2-Hydroxy-2,4,6-cycloheptatrien-1-one (tropolone **12**) possesses hydroxyl group alpha to the carbonyl group and is expected to exhibit keto-enol tautomerism. Interestingly, this compound exists almost exclusively in the enol form (**12A**), which possess resonance stabilization because of its aromaticity. Density functional theory calculations of the keto-enol



**Scheme 2** Synthesis of 6-isopropyl-thiotropolone (**10**) and 4-isopropyl-thiotropolone (**11**).



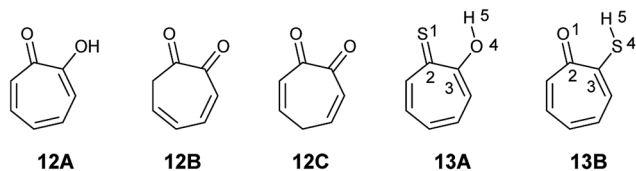


Fig. 4 Hydroxytropolone tautomers (12A–C) and mercaptotropolone tautomers (13A and B).

equilibrium constants of 2-hydroxy-2,4,6-cycloheptatrien-1-one (12A) and 3,5- and 3,6-cycloheptadiene-1,2-dione (12B and 12C) showed that the equilibrium is tilted in favour of the enol (12A) (Fig. 4).<sup>21</sup>

The corresponding thiotropolones have seven possible tautomers. The tautomeric equilibrium of all tautomers of thiotropolone was studied using Hartree Fock (HF) and density functional theory (B3LYP) at different levels of theory.<sup>22</sup> Calculating electronic energy and Gibbs free energy showed that the enol forms were more stable than the keto forms because of its aromaticity. This observation was supported by calculating the nucleus independent chemical shifts of NMR chemical shifts of the studied thiotropolones.<sup>22</sup> Compound 13A (2-hydroxy-2,4,6-cycloheptatriene-1-thione) was the most stable followed by compound 13B (2-mercapto-2,4,6-cycloheptatrien-1-one). The low energy of these two isomers is attributed to the favourable interactions between H5-S1 in 13A and H5-O1 in 13B.<sup>22</sup>

Nozoe *et al.*<sup>23</sup> was the first to synthesize 2-mercaptotropone and it was suggested to exist in two tautomeric forms. Sulfur-substituted derivatives were obtained upon alkylation and acylation of this compound, which suggests that 2-mercaptotropone (13B) is the prevailing tautomer. However, studying the physicochemical properties of 2-mercaptotropone and its structural analogues 6-isopropyl-2-mercaptotropone (10) and 4-isopropyl-2-mercaptotropone (11) in depth suggested that the major tautomer is the 2-hydroxyl trophthione (13A).<sup>24</sup>

Table 2 Experimental and calculated <sup>1</sup>H and <sup>13</sup>C NMR chemical shifts (ppm) of compound 10

Atom	$\delta_{\text{Exp}}$ 10A	$\delta_{\text{Calc}}$ 10A	$\delta_{\text{Calc}}$ 10B	Atom	$\delta_{\text{Exp}}$ 10A	$\delta_{\text{Calc}}$ 10A	$\delta_{\text{Calc}}$ 10B
C-1	183.4	210.3	180.0	H-3	7.45	6.71	7.48
C-2	172.5	179.0	185.9	H-4	—	—	—
C-3	119.6	118.2	141.2	H-5	7.21	6.98	7.07
C-4	161.2	164.9	164.1	H-6	7.14	6.88	7.18
C-5	132.1	132.6	133.9	H-7	8.45	8.98	8.08
C-6	133.8	130.9	136.8	H-8	2.91	2.62	2.91
C-7	143.0	159.8	130.8	H <sub>3</sub> -9	1.27	1.46	1.42
C-8	38.8	47.8	47.9	H <sub>3</sub> -10	1.27	1.45	1.47
C-9	23.4	26.9	25.2	OH or SH	9.50	8.98	4.04
C-10	23.4	24.3	24.0				

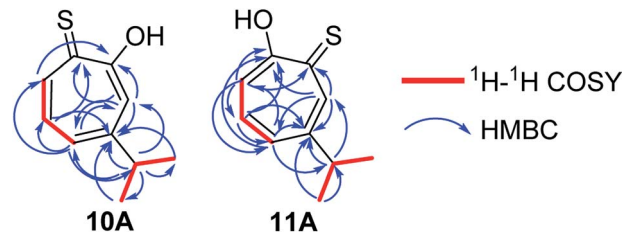
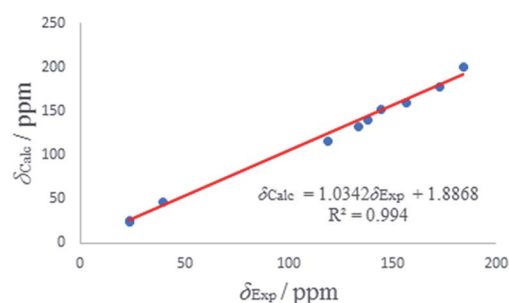


Fig. 5 Key <sup>1</sup>H-<sup>1</sup>H COSY and HMBC correlations of 10A and 11A.

Compound 10 was obtained as a dark red oil. Its molecular formula (C<sub>10</sub>H<sub>11</sub>OS)<sub>2</sub>Na<sup>+</sup> was determined by HRESIMS data (*m/z* 381.0951 [M<sub>2</sub> + Na]<sup>+</sup>, calc. 381.0953). The <sup>1</sup>H NMR showed that this compound exist in CDCl<sub>3</sub> as two tautomers 10A (≈ 87%) and 10B (≈ 13%). We were able to fully assign the chemical shifts of the major tautomer 10A (Table 2). The analysis of <sup>1</sup>H, <sup>13</sup>C, COSY, HSQC, and HMBC spectra revealed the presence of a singlet proton H-3 ( $\delta_{\text{C}}/\delta_{\text{H}}$  119.6/7.45, C-3). This proton shows two bond correlations with C-2 ( $\delta_{\text{C}}$  172.5) and C-4 ( $\delta_{\text{C}}$  161.2) and strong three bond correlations with C-1 ( $\delta_{\text{C}}$  183.4), C-5 ( $\delta_{\text{C}}$  132.1) and C-8 ( $\delta_{\text{C}}$  38.8). Furthermore, the one methine septet H-8 ( $\delta_{\text{C}}/\delta_{\text{H}}$  133.8/2.91, C-8) shows two bond correlations to C-4, C-9 and C-10 ( $\delta_{\text{C}}$  23.4) and three bond correlations to C-3 and C-5. The two-methyl doublet H<sub>3</sub>-9 and H<sub>3</sub>-10 ( $\delta_{\text{C}}/\delta_{\text{H}}$  23.4/1.27, C-9 and C-10) shows two bond correlations to C-8 and a strong three bond correlation to C-4. H-5 ( $\delta_{\text{C}}/\delta_{\text{H}}$  132.1/7.21, C-5) shows two bond correlations to C-6, and strong three bond correlations to C-3, C-7 and C-8. H-6 ( $\delta_{\text{C}}/\delta_{\text{H}}$  133.8/7.14, C-3) shows strong three bond correlations to C-1 and C-4. H-7 ( $\delta_{\text{C}}/\delta_{\text{H}}$  143.0/8.45, C-7) shows strong three bond correlations to C-2 and C-5 (Fig. 5).

A.



B.

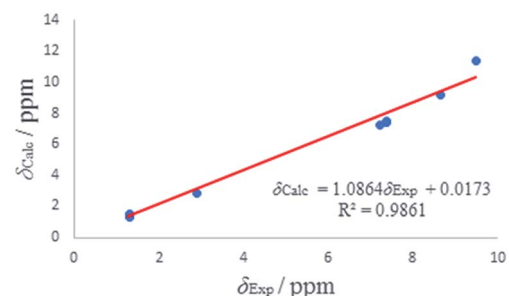
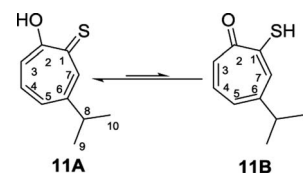


Fig. 6 (A) Experimental <sup>13</sup>C chemical shifts ( $\delta$ ) of 10A (vs.) calculated. (B) Experimental <sup>1</sup>H chemical shifts ( $\delta$ ) of 10A (vs.) calculated.





**Table 3** Experimental and calculated  $^1\text{H}$  and  $^{13}\text{C}$  NMR chemical shifts (ppm) of compound **11**

							
Atom	$\delta_{\text{Exp}}$ <b>11A</b>	$\delta_{\text{Calc}}$ <b>11A</b>	$\delta_{\text{Calc}}$ <b>11B</b>	Atom	$\delta_{\text{Exp}}$ <b>11A</b>	$\delta_{\text{Calc}}$ <b>11A</b>	$\delta_{\text{Calc}}$ <b>11B</b>
C-1	184.1	202.0	181.5	H-3	7.34	7.50	7.29
C-2	172.2	179.8	185.5	H-4	7.35	7.54	7.51
C-3	118.2	117.1	138.3	H-5	7.19	7.34	7.07
C-4	137.9	142.0	140.4	H-6	—	—	—
C-5	133.0	134.3	131.1	H-7	8.62	9.32	8.27
C-6	156.5	161.1	163.3	H-8	2.88	2.94	2.91
C-7	144.0	152.8	135.2	H <sub>3</sub> -9	1.27	1.47	1.51
C-8	39.0	47.8	47.7	H <sub>3</sub> -10	1.27	1.51	1.44
C-9	23.1	26.4	24.0	OH or SH	9.47	11.46	4.10
C-10	23.1	25.4	28.1				

We have calculated both  $^1\text{H}$  and  $^{13}\text{C}$  isotropic chemical shielding of **10A** and **10B** at the B3LYP/def2-TZVPP level of theory. Correlation plots between experimental and calculated chemical shifts shows very good correlations in case of **10A** with  $R^2$  of 0.9828 and 0.99 for  $^{13}\text{C}$  and  $^1\text{H}$  NMR chemical shifts, respectively (Fig. 6). The calculated chemical shift values of isomer **10B** correlated to less extent with the experimental values (see Fig. S52†).

Compound **11** was obtained as orange microcrystals. Its molecular formula  $(\text{C}_{10}\text{H}_{11}\text{OS})_2\text{Na}^+$  was determined by HRESIMS data ( $m/z$  381.0950  $[\text{M}_2 + \text{Na}]^+$ , calc. 381.0953). This compound exists in  $\text{CDCl}_3$  as a mixture of two tautomers **11A** ( $\approx 96\%$ ) and **11B** ( $\approx 4\%$ ). We were able to fully assign the chemical shifts of the major tautomer **11A** (Table 3). The analysis of  $^1\text{H}$ ,  $^{13}\text{C}$ , COSY, HSQC, and HMBC spectra revealed the presence of a singlet proton H-7 ( $\delta_{\text{C}}/\delta_{\text{H}}$  144.0/8.62, C-7). This proton shows two bond correlations with C-1 ( $\delta_{\text{C}}$  184.1) and C-6 ( $\delta_{\text{C}}$  156.5) and strong three bond correlations with C-2 ( $\delta_{\text{C}}$  172.2) and C-5 ( $\delta_{\text{C}}$  133.0). Furthermore, the one methine septet H-8 ( $\delta_{\text{C}}/\delta_{\text{H}}$  39.0/2.88, C-8) shows two bond correlations to C-6 ( $\delta_{\text{C}}$  156.5) and three bond correlations to C-7. The two-methyl doublet H<sub>3</sub>-9 and H<sub>3</sub>-10 ( $\delta_{\text{C}}/\delta_{\text{H}}$  23.1/1.27, C-9 and C-10) shows two bond correlations to C-8 and a strong three bond correlation to C-6. H-5 ( $\delta_{\text{C}}/\delta_{\text{H}}$  133.0/7.19, C-5) shows two bond correlations to C-6, strong three bond correlations to C-3 and C-8, and four bond correlations to C-2. H-3 ( $\delta_{\text{C}}/\delta_{\text{H}}$  118.2/7.34, C-3) shows two bond correlations to C-2 and C-4 and strong three bond correlations to C-1 and C-5. H-4 ( $\delta_{\text{C}}/\delta_{\text{H}}$  137.9/7.35, C-4) shows two bond correlations to C-5 and strong three bond correlations to C-2 and C-6 which further confirms the location of the isopropyl groups (Fig. 5).

$^1\text{H}$  and  $^{13}\text{C}$  isotropic chemical shielding of **11A** and **11B** were calculated at the B3LYP/def2-TZVPP level of theory (Table 3). Correlation plots between experimental and calculated chemical shifts shows very good correlations in the case of **11A**, with  $R^2$  of 0.994 and 0.9861 for  $^{13}\text{C}$  and  $^1\text{H}$  NMR chemical shifts, respectively (Fig. 7). The calculated

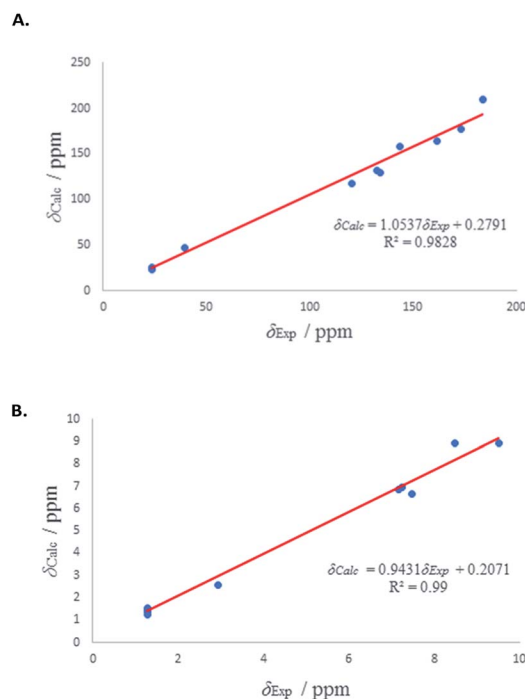


**Fig. 7** (A) Experimental  $^{13}\text{C}$  chemical shifts ( $\delta$ ) of **11A** (vs.) calculated. (B) Experimental  $^1\text{H}$  chemical shifts ( $\delta$ ) of **11A** (vs.) calculated.

chemical shift values of isomer **11B** correlated to less extent with the experimental values (see Fig. S53†).

### Computational details

Electronic structure calculations were performed using ORCA.<sup>25,26</sup> Crystal structures of compounds **8** and **9** were optimized at the DFT theory BLYP with basis sets def2-SVP and RI approximation. Geometries of compounds **10** and **11**, and their isomers were modelled using the Avogadro program.<sup>27</sup> Their geometries were



Table 4 MIC<sub>80</sub> and CC<sub>50</sub> values against *E. coli*, *S. aureus*, *A. baumannii*, *P. aeruginosa*, and *C. neoformans*

Comp.	Bacteria MIC <sub>80</sub> (μM)					CC <sub>50</sub>	
	<i>S. aureus</i> (29213)	<i>E. coli</i> (35218)	<i>A. baumannii</i> (from a patient)	<i>P. aeruginosa</i> (27853)	<i>C. neoformans</i> MIC <sub>80</sub>	CC <sub>50</sub> (neutral red)	CC <sub>50</sub> (MTS)
<b>2</b> <sup>d</sup>	66.7	44.4	51.2	>100	21 (ref. 4)	na	66.4
<b>8</b>	>100	>100	>100	>100	24	31.8	33.6
<b>9</b>	8.8	>100	>100	>100	24	19.5	34.2
<b>10</b>	>100	>100	>100	>100	50	39.7	95
<b>11</b>	16	>100	>100	>100	24	30.4	64.2

Table 5 Calculated molecular descriptors for prediction of ADME properties for each compound. Recommended values or range for 95% of known drugs is shown in parenthesis

Comp.	<sup>a</sup> mol_MW	<sup>b</sup> QP log Po/w	<sup>c</sup> HBD	<sup>d</sup> HBA	<sup>e</sup> % Human oral absorption	<sup>f</sup> PSA	<sup>g</sup> Qp log S	<sup>h</sup> QPPCaco	<sup>i</sup> #Metab	<sup>j</sup> Qp log BB	<sup>k</sup> QPPMDCK
<b>2</b>	164.204	1.443	1	2.75	89.394	50.125	−2.193	1040.346	2	−0.396	516.318
<b>8</b>	318.387	2.1	0	6.5	92.748	68.778	−2.742	975.826	2	−0.615	490.424
<b>9</b>	318.387	2.216	0	6.5	94.321	68.77	−2.952	1095.291	2	−0.591	555.56
<b>10A</b>	180.264	2.351	0.8	2.5	100	28.102	−2.794	3286.638	2	0.207	4437.612
<b>10B</b>	180.264	2.4	1	2.25	100	29.939	−2.881	3010.296	2	0.168	3962.203
<b>11A</b>	180.264	2.36	0.8	2.5	100	28.166	−2.843	3222.618	2	0.195	4334.35
<b>11B</b>	180.264	2.398	1	2.25	100	30.01	−2.884	2998.094	2	0.166	3935.7

<sup>a</sup> Molar weight in Daltons (130–725). <sup>b</sup> Logarithm of partitioning coefficient between *n*-octanol and water phases (range for 95% of drugs: −2 to 6). <sup>c</sup> Number of hydrogen bonds donors (0–6). <sup>d</sup> Number of hydrogen bond acceptors (2–20). <sup>e</sup> Predicted human oral absorption on a 0–100% scale, based on a multiple linear regression model (<25% low, >80% high). <sup>f</sup> Polar surface area (7–200). <sup>g</sup> Predicted aqueous solubility, log S in mol dm<sup>−3</sup> (−6.5 to 0.5). <sup>h</sup> Predicted apparent Caco-2 cell permeability in nm s<sup>−1</sup> as a model for the gut-blood barrier (<25 poor, >500 excellent). <sup>i</sup> Number of possible metabolic reactions (2–8). <sup>j</sup> Predicted brain/blood partition coefficient (−3 to 1.2). <sup>k</sup> Predicted apparent MDCK cell permeability in nm s<sup>−1</sup> as a mimic for blood/brain barrier (<25 poor, >500 excellent). Qikrop predictions are for non-active transport.

optimized at the B3LYP functional<sup>28,29</sup> and def2-TZVPP basis set.<sup>30</sup> The RjCosX approximation and def2/J auxiliary basis set were used during optimization. The absolute <sup>1</sup>H NMR chemical shifts ( $\delta_{\text{H}}$ ), <sup>13</sup>C NMR chemical shifts ( $\delta_{\text{C}}$ ) for all compounds were calculated with the GIAO (Gauge Including Atomic Orbitals) method<sup>31–33</sup> at B3LYP def2-TZVPP level of theory. The TMS shielding was calculated at the same level of theory and relative chemical shifts were then estimated by subtracting the calculated chemical shift from TMS. The calculated <sup>1</sup>H and <sup>13</sup>C isotropic chemical shielding of TMS are 31.942/183.923.

### Biological evaluation

The broad anti-bacterial activity of  $\beta$ -thujaplicin (Hinokitiol, **2**) was reported several decades ago.<sup>34,35</sup> Compound **2** could modestly inhibit *S. aureus*, *E. coli*, and *A. baumannii* in our experimental conditions, with MIC<sub>80</sub> values of 66.7, 44.4 and 51.2 μM, respectively. Compound **8**, which is the rearranged tosyl isomer of the natural product **2**, has no activity against all tested bacteria (MIC<sub>80</sub> > 100 μM). However, this compound showed similar activity to **2** against *C. neoformans* (MIC<sub>80</sub> = 24 μM for **8** vs. MIC<sub>80</sub> = 21 μM for **2**). Interestingly, compound **9**, which is the tosylated derivative of the natural product **2** showed 8-fold increase in the antibacterial activity against *S. aureus*, but diminished activity against the Gram-negative bacteria *E. coli*, *A. baumannii*, and *P. aeruginosa*. Compound **9** has similar activity to **2** and **8** against *C. neoformans* (MIC<sub>80</sub> = 24 μM) (Table 4).

The mercapto derivative of **8**, compound **10**, has no anti-bacterial activity against all four tested bacteria. The activity of **10** against *C. neoformans* (MIC<sub>80</sub> = 50 μM) is >2-fold less than the corresponding hydroxy tropolone **2**. The mercapto derivative of **9**, compound **11**, which is the direct isomer of **2**, showed promising antibacterial activity against *S. aureus* (MIC<sub>80</sub> = 16 μM), but no activity against the other tested bacteria. Compound **11** showed similar activity as **2**, **8**, and **9** against *C. neoformans* (MIC<sub>80</sub> = 24 μM) (Table 4).

We tested the cytotoxicity of the synthesized compounds in hepatoblastoma cells using an MTS cytotoxicity assay that measures mitochondrial function and a neutral red assay that measures lysosomal function and calculated the CC<sub>50</sub>, which is the concentration of inhibitor required to reduce cell viability 50% relative to untreated cells (Table 4). Compound **10** have the lowest toxicity among all synthesized compounds in both assays. The toxicity of compound **11** is relatively low, and comparable to the natural product  $\beta$ -thujaplicin (**2**).

### In silico ADME evaluation

We calculated a set of physical descriptors and pharmaceutical properties of all tested compounds using Qikprop to predict their absorption, distribution, metabolism, and excretion (ADME) properties (Table 5). All compounds are in compliance with Lipinski's rule of five<sup>36</sup> and Jorgensen's rule of three<sup>37</sup> and



are predicted to have good oral bioavailability and excellent absorption through cell membranes.

## Conclusions

Tosylated thujaplicin isomers **8** and **9** were separated for the first time and their structures were fully characterized. Isomers **8** and **9** were used to synthesize the two mercapto isomers of  $\beta$ -thujaplicin, **10** and **11**, in a regioselective manner.  $^1\text{H}$  and  $^{13}\text{C}$  Chemical shifts of synthesized isomers were fully assigned using several NMR experiments, and their isotropic magnetic shielding was calculated computationally. The calculated chemical shift values were in a good agreement with the experimental results. When the biological activity of the synthesized compounds was evaluated against *C. neoformans* and four different bacterial strains, 4-isopropyl-thiotropolone (**11**) displayed good potency against *Staphylococcus aureus* (ATCC 29213). The relatively non-toxic nature of this compound and excellent predicted ADME properties make it a potential lead compound to develop potent inhibitors against *Staphylococcus aureus* infection.

## Experimental section

All materials were purchased from commercial suppliers and used without further purification. Purification was done by Reveleris X2 flash chromatography. The purities of the final compounds were characterized by high-performance liquid chromatography (HPLC) using a gradient elution program (Ascentis Express Peptide C18 column, acetonitrile/water 5/95  $\rightarrow$  95/5, 5 min, 0.05% trifluoroacetic acid) and UV detection (254 nm). The purities of final compounds were 95% or greater. NMR spectra was recorded on a Bruker NMR 400 MHz Avance III spectrometer operating at 400 MHz for  $^1\text{H}$  NMR and 100 MHz for  $^{13}\text{C}$  NMR. Chemical shifts are given in part per million (ppm) relative to tetramethylsilane (TMS), coupling constants  $J$  are given in Hertz. High-resolution mass spectra were obtained using electrospray ionization on a Bruker 12 T APEX-Qe FTICR-MS with an Apollo II ion source at the COSMIC Laboratory facility at Old Dominion University, VA.

### Synthesis of compounds **8** and **9**

*p*-Toluenesulfonyl chloride (2.3 g, 12.2 mmol) was added to a solution of tropolone (2 g, 12.2 mmol) and DIPEA (4.3 mL, 24.4 mmol) in DCM (50 mL), and the reaction mixture was stirred overnight. The resulting mixture was successively washed with 1 M HCl (30 mL), water (30 mL) and brine (30 mL). The organic layer was dried over  $\text{Na}_2\text{SO}_4$ , filtered and the solvent was evaporated *in vacuo* yielding a mixture of the two isomers, which were separated by flash chromatography using (EtOAc/hexanes 3 : 7) with a flow rate 10 mL  $\text{min}^{-1}$  to obtain each isomer in a pure form.

### 6-(1-Methylethyl)-2-[[[4-methylphenyl)sulfonyl]oxy]-2,4,6-cycloheptatrien-1-one (**8**)

White needles (46%),  $R_f = 0.655$  (EtOAc/hexanes 1 : 1).  $^1\text{H}$  NMR (400 MHz, chloroform- $d$ )  $\delta$  7.92 (d,  $J = 7.3$  Hz, 2H), 7.38–7.26 (m,

3H), 7.08 (s, 1H), 7.01 (d,  $J = 11.4$  Hz, 1H), 6.91 (t,  $J = 10.3$  Hz, 1H), 2.82–2.67 (m, 1H), 2.44 (s, 3H), 1.20 (d,  $J = 6.7$  Hz, 6H);  $^{13}\text{C}$  NMR (100 MHz, chloroform- $d$ )  $\delta$  179.2, 157.5, 154.6, 145.4, 137.8, 136.7, 133.5, 129.7, 129.6, 129.3, 128.6, 38.4, 22.7, 21.8; LC/MS  $m/z$ : 319.1  $[\text{M} + \text{H}]^+$ , 341  $[\text{M} + \text{Na}]^+$ . HRESIMS  $m/z$  341.0816  $[\text{M} + \text{Na}]^+$  (calcd for  $\text{C}_{17}\text{H}_{18}\text{O}_4\text{SNa}^+$ , 341.0818).

### 4-(1-Methylethyl)-2-[[[4-methylphenyl)sulfonyl]oxy]-2,4,6-cycloheptatrien-1-one (**9**)

White powder (43%),  $R_f = 0.483$  (EtOAc/hexanes 1 : 1).  $^1\text{H}$  NMR (400 MHz, chloroform- $d$ )  $\delta$  7.93 (d,  $J = 7.6$  Hz, 2H), 7.41–7.32 (m, 3H), 7.17 (dd,  $J = 12.1, 8.7$  Hz, 1H), 7.04 (d,  $J = 12.3$  Hz, 1H), 6.96 (d,  $J = 8.6$  Hz, 1H), 2.89–2.75 (m, 1H), 2.46 (s, 3H), 1.24 (d,  $J = 6.8$  Hz, 6H);  $^{13}\text{C}$  NMR (100 MHz, chloroform- $d$ )  $\delta$  178.9, 154.5, 152.4, 145.5, 139.0, 136.9, 133.4, 131.8, 130.5, 129.6, 128.6, 38.1, 22.8, 21.8; LC/MS  $m/z$ : 319.1  $[\text{M} + \text{H}]^+$ , 341  $[\text{M} + \text{Na}]^+$ . HRESIMS  $m/z$  341.0815  $[\text{M} + \text{Na}]^+$  (calcd for  $\text{C}_{17}\text{H}_{18}\text{O}_4\text{SNa}^+$ , 341.0818).

### General procedure for the synthesis of **10** and **11**

NaSH (0.122 g, 2.17 mmol) was added portion wise to a solution of **8** or **9** (0.150 g, 0.54 mmol) in ethanol (10 mL). The reaction mixture was stirred for 2 h at room temperature and was monitored by LCMS and TLC till completion. Ethanol was evaporated, and the resulting solid was dissolved in water and acidified with HCl (2 M) then extracted with DCM (3  $\times$  20 mL) to yield the desired product. Purification was performed by flash chromatography using a mixture of EtOAc/hexanes to obtain the desired compound.

### 2-Hydroxy-4-isopropylcyclohepta-2,4,6-triene-1-thione (**10**)

Red dark oil,  $R_f = 0.876$  (EtOAc/hexanes 1 : 1).  $^1\text{H}$  NMR (400 MHz, chloroform- $d$ )  $\delta$  9.71 (s, 1H), 8.46 (d,  $J = 10.6$  Hz, 1H), 7.47 (s, 1H), 7.23 (d,  $J = 9.7$  Hz, 1H), 7.16 (t,  $J = 10.2$  Hz, 1H), 2.99–2.87 (m, 1H), 1.29 (d,  $J = 6.9$  Hz, 7H);  $^{13}\text{C}$  NMR (101 MHz,  $\text{CDCl}_3$ )  $\delta$  183.5, 172.5, 161.4, 143.1, 134.0, 132.2, 119.7, 38.9, 23.5; LC/MS  $m/z$ : 181  $[\text{M} + \text{H}]^+$ . HRESIMS  $m/z$  381.0951  $[\text{M}_2 + \text{Na}]^+$  (calcd for  $(\text{C}_{10}\text{H}_{11}\text{OS})_2\text{Na}^+$ , 381.0953).

### 7-Hydroxy-3-isopropylcyclohepta-2,4,5-triene-1-thione (**11**)

Orange crystal,  $R_f = 0.793$ , (EtOAc/hexanes 1 : 1).  $^1\text{H}$  NMR (400 MHz, chloroform- $d$ )  $\delta$  9.86 (s, 1H), 8.63 (s, 1H), 7.39–7.26 (m, 2H), 7.26–7.11 (m, 1H), 2.94–2.83 (m, 1H), 1.27 (d,  $J = 6.9$  Hz, 6H);  $^{13}\text{C}$  NMR (101 MHz,  $\text{CDCl}_3$ )  $\delta$  184.3, 172.2, 156.6, 144.1, 138.0, 133.1, 118.3, 39.1, 23.5; LC/MS  $m/z$ : 181  $[\text{M} + \text{H}]^+$ . HRESIMS  $m/z$  381.0950  $[\text{M}_2 + \text{Na}]^+$  (calcd for  $(\text{C}_{10}\text{H}_{11}\text{OS})_2\text{Na}^+$ , 381.0953).

### X-ray structure determination of **8**

A crystals of approximate dimensions  $0.544 \times 0.254 \times 0.132$   $\text{mm}^3$  was mounted on a MiTeGen cryoloop in a random orientation. Preliminary examination and data collection were performed using a Bruker X8 Kappa Apex II Charge Coupled Device (CCD) Detector system single crystal X-ray diffractometer equipped with an Oxford Cryostream LT device. All data were collected using graphite monochromated Mo K radiation ( $\lambda = 0.71073$  Å) from a fine focus sealed tube X-ray source.



Preliminary unit cell constants were determined with a set of 36 narrow frame scans. Typical data sets consist of combinations of  $\omega$  and  $\phi$  scan frames with typical scan width of 0.5 and counting time of 10 seconds per frame at a crystal to detector distance of 4.0 cm. The collected frames were integrated using an orientation matrix determined from the narrow frame scans. Apex II and SAINT software packages (Bruker Analytical X-ray, Madison, WI, 2016) were used for data collection and data integration. Analysis of the integrated data did not show any decay. Final cell constants were determined by global refinement of 7781 reflections harvested from the complete data set. Collected data were corrected for systematic errors using SADABS (Bruker Analytical X-ray, Madison, WI, 2016) based on the Laue symmetry using equivalent reflections.

Crystal data and intensity data collection parameters are listed in Table 1S.† Structure solution and refinement were carried out using the SHELXTL-PLUS software package.<sup>40</sup> The structure was solved and refined successfully in the monoclinic space group  $P2_1/c$ . Full matrix least-squares refinements were carried out by minimizing  $w(F_o^2 - F_c^2)^2$ . The non-hydrogen atoms were refined anisotropically to convergence. The 7-membered ring is disordered, and the two orientations were refined with geometrical restraints to 82 : 18%. All hydrogen atoms were treated using appropriate riding model (AFIX m3). The final residual values and structure refinement parameters are listed in Table 1S.†

Complete listings of positional and isotropic displacement coefficients for hydrogen atoms, anisotropic displacement coefficients for the non-hydrogen atoms and other geometrical parameters are listed as ESI (Tables 2S to 7S†). Table of calculated and observed structure factors are available in electronic format.

### Bacterial strains

*Staphylococcus aureus* (ATCC 29213), *Escherichia coli* (ATCC 35218), and *Pseudomonas aeruginosa* (ATCC 27853) were obtained from the American Type Culture Collection (ATCC). *Acinetobacter baumannii* was collected from the microbiology laboratory at the John Cochran division of the St. Louis VA Medical Center (STLVAMC) under a Subcommittee on Research Safety (SRS)-approved protocol.

### Determination of the minimum inhibitory concentration

MIC<sub>80</sub>s were determined by the broth microdilution method recommended by the Clinical and Laboratory Standards Institute (CLSI) in cation-adjusted Mueller–Hinton II broth (CAMHB). A 1.5-fold dilution series of the compounds was prepared in CAMHB. Overnight bacterial culture was added to the diluted compounds in a 96 well plate after adjusting the bacterial concentration to  $5 \times 10^5$  CFU mL<sup>-1</sup> in final concentration. After 16–24 hours incubation at 35 °C  $\pm$  2 °C, the plates were read at 600 nM in microplate reader. The MIC<sub>80</sub> was defined as the concentration of an antibacterial agent that inhibited bacteria growth  $\geq$ 80% compared to vehicle-treated control cultures. All values were determined at least twice independently, and the average number is reported.

### Inhibition of *C. neoformans* growth

Compounds were tested *C. neoformans* var *grubii*, KN99 (serotype A, MAT $\alpha$ ) in a limiting dilution assay with a starting optical density (650 nM) of 0.001 in YNB-02 (0.67% yeast nitrogen base, 0.2% dextrose, pH 7.0 with 50 mM MOPs) + 1% DMSO. Cells were incubated without shaking for 48 hours at 35 °C and cell density was measured at 650 nM. The minimal inhibitory concentration was determined using compound concentrations from 0.19 to 50  $\mu$ M of the compound in YNB-02 + 1% DMSO. Each assay was done in triplicate and all values are the average of two or more independent assays. The data are presented as the average cell density as a percent of DMSO-only treated cells. MICs are reported as the minimal concentration needed to inhibit 80% of *C. neoformans* growth relative to vehicle-treated controls.

### Cytotoxicity in hepatoma cells

HepDES19 cells<sup>38</sup> ( $1.0 \times 10^4$  cells per well) were seeded in 96-well plates and incubated in Dulbecco's Modified Eagle Medium (DMEM) with 10% FBS plus 1% penicillin/streptomycin solution, 1% nonessential amino acids, and 1% glutamine. The compounds were diluted in the medium to the desired concentrations at a final concentration of 1% DMSO and added to the cells 48 h after plating, with each concentration tested in triplicate.

### MTS cytotoxicity assay (CC<sub>50</sub>)

Soluble MTS reagent [3-(4,5-dimethylthiazol-2-yl)-5-(3-carboxymethoxyphenyl)-2-(4-sulfophenyl)-2H-tetrazolium, Promega] was added 72 h after incubation, the cultures were incubated for 90 min, and absorbance was read at 490 nm. The CC<sub>50</sub> was calculated as the concentration of inhibitor required to reduce cell viability 50% relative to untreated cells. The data are plotted as log[inhibitor] *versus* response and fit to a variable slope model using GraphPad Prism (v6, www.graphpad.com).<sup>4</sup>

### Neutral red assay (CC<sub>50</sub>)

Cells were incubated with the compound for 72 hours and cytotoxicity was measured using a neutral red assay.<sup>39</sup> The data were transformed to log[inhibitor] and fit to a 4-variable slope curve using GraphPad Prism. The concentration at which 50% of cells were inhibited relative to vehicle-treated control is reported as the CC<sub>50</sub> value.

## Conflicts of interest

There are no conflicts to declare.

## Acknowledgements

This work was financially supported by Saint Louis University Start up fund (No. 203437). Funding from the National Science Foundation (MRI, CHE-0420497) for the purchase of the Apex-II diffractometer is acknowledged. We would like to thank Ms Ashley Anderson for help with acquiring NMR.





## Notes and references

- 1 M. Yamato, K. Hashigaki, Y. Yasumoto, J. Sakai, R. F. Luduena, A. Banerjee, S. Tsukagoshi, T. Tashiro and T. Tsuruo, *J. Med. Chem.*, 1987, **30**, 1897–1900.
- 2 K. Sugawara, M. Ohbayashi, K. Shimizu, M. Hatori, H. Kamei, M. Konishi, T. Oki and H. Kawaguchi, *J. Antibiot.*, 1988, **41**, 862–868.
- 3 M. Yamato, J. Ando, K. Sakaki, K. Hashigaki, Y. Wataya, S. Tsukagoshi, T. Tashiro and T. Tsuruo, *J. Med. Chem.*, 1992, **35**, 267–273.
- 4 M. J. Donlin, A. Zunica, A. Lipnicky, A. K. Garimallaprabhakaran, A. J. Berkowitz, A. Grigoryan, M. J. Meyers, J. E. Tavis and R. P. Murelli, *Antimicrob. Agents Chemother.*, 2017, **61**, e02574-16.
- 5 W. H. Johnston, J. J. Karchesy, G. H. Constantine and A. M. Craig, *Phytother. Res.*, 2001, **15**, 586–588.
- 6 S. R. Piettre, A. Ganzhorn, J. Hoflack, K. Islam and J. M. Hornsperger, *J. Am. Chem. Soc.*, 1997, **119**, 3201–3204.
- 7 D. M. Himmel, K. A. Maegley, T. A. Pauly, J. D. Bauman, K. Das, C. Dharia, A. D. Clark, K. Ryan, M. J. Hickey, R. A. Love, S. H. Hughes, S. Bergqvist and E. Arnold, *Structure*, 2009, **17**, 1625–1635.
- 8 S. J. Newberry, J. D. FitzGerald, A. Motala, M. Booth, M. A. Maglione, D. Han, A. Tariq, C. E. O'Hanlon, R. Shanman, W. Dudley and P. G. Shekelle, *Ann. Intern. Med.*, 2017, **166**, 27–36.
- 9 S. Özen, E. D. Batu and S. Demir, *Front. Immunol.*, 2017, **8**, 253.
- 10 A. Bayes-Genis, Y. Adler, A. B. De Luna and M. Imazio, *Eur. Heart J.*, 2017, **38**, 1706–1709.
- 11 H. Yamano, T. Yamazaki, K. Sato, S. Shiga, T. Hagiwara, K. Ouchi and T. Kishimoto, *Antimicrob. Agents Chemother.*, 2005, **49**, 2519–2521.
- 12 A. Muzaffar, A. Brossi, C. M. Lin and E. Hamel, *J. Med. Chem.*, 1990, **33**, 567–571.
- 13 J. Guan, X. K. Zhu, Y. Tachibana, K. F. Bastow, A. Brossi, E. Hamel and K. H. Lee, *J. Med. Chem.*, 1998, **41**, 1956–1961.
- 14 S. Tsubotani, Y. Wada, K. Kamiya, H. Okazaki and S. Harada, *Tetrahedron Lett.*, 1984, **25**, 419–422.
- 15 K. Kintaka, H. Ono, S. Tsubotani, S. Harada and H. Okazaki, *J. Antibiot.*, 1984, **37**, 1294–1300.
- 16 I. Tamburlin-Thumin, M. P. Crozet, J. C. Barriere, M. Barreau, J. F. Riou and F. Lavelle, *Eur. J. Med. Chem.*, 2001, **36**, 561–568.
- 17 M. Cavazza and F. Pietra, *Org. Biomol. Chem.*, 2003, **1**, 3002–3003.
- 18 M. C. Barret, P. H. Bhatia, G. Kociok-Köhn and K. C. Molloy, *Transition Met. Chem.*, 2014, **39**, 543–551.
- 19 T. Yanagisawa, K. Kosakai, T. Tomiyama, M. Yasunami and K. Takase, *Chem. Pharm. Bull.*, 1990, **38**, 3355–3358.
- 20 M. Cavazza and F. Pietra, *Tetrahedron Lett.*, 2003, **44**, 1895–1897.
- 21 S. W. Paine and A. Salam, *Chem. Phys.*, 2006, **331**, 61–66.
- 22 S. W. Paine and A. Salam, *Int. J. Quantum Chem.*, 2012, **113**, 1245–1252.
- 23 T. Nozoe, M. Satô and K. Matsui, *Proc. Jpn. Acad.*, 1953, **29**, 22–26.
- 24 T. Nozoe and K. Matsui, *Bull. Chem. Soc. Jpn.*, 1961, **34**, 616–618.
- 25 N. Frank, *Wiley Interdiscip. Rev.: Comput. Mol. Sci.*, 2011, **2**, 73–78.
- 26 N. Frank, *Wiley Interdiscip. Rev.: Comput. Mol. Sci.*, 2017, **8**, e1327.
- 27 M. D. Hanwell, D. E. Curtis, D. C. Lonie, T. Vandermeersch, E. Zurek and G. R. Hutchison, *J. Cheminf.*, 2012, **4**, 17.
- 28 A. D. Becke, *J. Chem. Phys.*, 1986, **84**, 4524–4529.
- 29 A. D. Becke, *J. Chem. Phys.*, 1993, **98**, 5648–5652.
- 30 F. Weigend and R. Ahlrichs, *Phys. Chem. Chem. Phys.*, 2005, **7**, 3297–3305.
- 31 F. London, *J. Phys. Radium*, 1937, **8**, 397–409.
- 32 R. Ditchfield, *J. Chem. Phys.*, 1972, **56**, 5688–5691.
- 33 T. Helgaker, M. Jaszuński and K. Ruud, *Chem. Rev.*, 1999, **99**, 293–352.
- 34 Y. Arima, Y. Nakai, R. Hayakawa and T. Nishino, *J. Antimicrob. Chemother.*, 2003, **51**, 113–122.
- 35 Y.-H. Shih, D.-J. Lin, K.-W. Chang, S.-M. Hsia, S.-Y. Ko, S.-Y. Lee, S.-S. Hsue, T.-H. Wang, Y.-L. Chen and T.-M. Shieh, *PLoS One*, 2014, **9**, e94941.
- 36 C. A. Lipinski, F. Lombardo, B. W. Dominy and P. J. Feeney, *Adv. Drug Delivery Rev.*, 2001, **46**, 3–26.
- 37 W. L. Jorgensen and E. M. Duffy, *Adv. Drug Delivery Rev.*, 2002, **54**, 355–366.
- 38 H. Guo, D. Jiang, T. Zhou, A. Cuconati, T. M. Block and J.-T. Guo, *J. Virol.*, 2007, **81**, 12472–12484.
- 39 G. Repetto, A. del Peso and J. L. Zurita, *Nat. Protoc.*, 2008, **3**, 1125.
- 40 G. M. Sheldrick, *Acta Crystallogr., Sect. A: Found. Crystallogr.*, 2008, **64**, 112–122.

